

# Investigating Mold Heat Transfer in Thin Slab Casting With CON1D

Mold heat transfer in continuous casting is important to mold life, surface quality, breakouts and many aspects of the process. Heat transfer in the thin slab casting mold is being investigated with the 1-D heat transfer model, CON1D. To account for the multi-dimensional thermal behavior around the cooling channels of the funnel mold, a three-dimensional finite element model, developed using ABAQUS, is applied to find correction factors that enable CON1D to predict accurately temperature at thermocouple locations. The model calculations have been validated using an extensive database of plant process parameters obtained from the Corus Direct Sheet Plant in IJmuiden, The Netherlands, including measurements of mold powder consumption, oscillation mark shape, mold temperature and heat removal. The improved CON1D model is applied here to predict casting behavior for different speeds and to investigate the effect of mold plate thickness. The results will be used to extrapolate standard practices to higher casting speeds and new mold designs.

## CON1D Model Description

The heat transfer model CON1D<sup>1</sup> models several aspects of the continuous casting process, including shell and mold temperatures, heat flux, interfacial microstructure and velocity, shrinkage estimates to predict taper, mold water temperature rise and convective heat transfer coefficient, interfacial friction and many other phenomena. The heat transfer calculations are one-dimensional through the thickness of the shell and interfacial gap with two-dimensional conduction calculations in the mold. An entire simulation requires only a few seconds on a modern PC.

Heat transfer in the mold is computed assuming a slab with attached rectangular blocks that form the cooling-water channels and act as heat transfer fins. The process

parameters used in this analysis are typical values used with the Corus Direct Sheet Plant (DSP) thin slab continuous casting machine in IJmuiden. Key parameters include casting

---

**A 3-D finite element model is applied to find factors that enable CON1D to predict temperature at thermocouple locations. The improved CON1D model is applied to predict casting behavior for different speeds and to investigate the effect of mold plate thickness.**

---

speeds of 4.5 and 5.2 m/minute, pour temperature of 1,545°C, meniscus level of 100 mm below the top of the funnel mold, casting a 0.045%C steel. To accurately model the complex geometry of the funnel mold and water slots, an offset methodology<sup>2</sup> is applied to calibrate the model to match the predictions of a full three-dimensional finite element model using ABAQUS.<sup>3</sup>

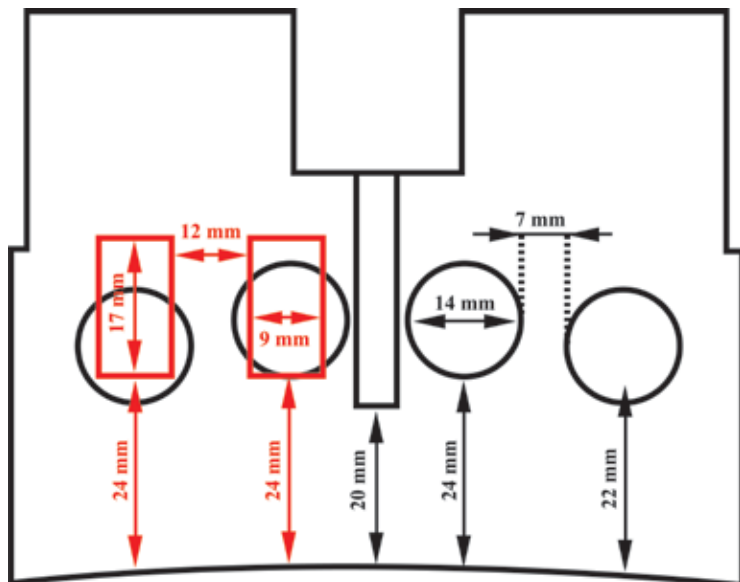
**Narrow Face** — To create the simple mold geometry for CON1D, the actual narrow face cross-section (black) was transformed into the one-dimensional rectangular channel geometry (red), as shown in Figure 1. The bolt holes are 22 mm in diameter and 20.5 mm deep; the thermocouple holes are 4 mm in diameter and extend into the mold such that they are 20 mm from the hot face.

To approximate the actual geometry, the shortest distance between the water channels and the hot face was maintained at 24 mm and the pitch between the channels similarly was set to 12 mm. To match the water flowrate, the dimensions of the rectangular channels were chosen to keep the cross-sectional area about the same as that of the actual 14-mm-diameter channels. In addition, to maintain heat

## Authors

**Begoña Santillana** (left), researcher, **Arie Hamoen** and **Willem van der Knoop**, Corus RD&T SCC/CMF, IJmuiden, The Netherlands (begona.santillana@corus-group.com, arie.hamoen@corusgroup.com, willem.van-der-knoop@corusgroup.com); **Brian G. Thomas** (center) and **Lance C. Hibbeler** (right), University of Illinois at Urbana-Champaign, Urbana, Ill. (bgthomas@uiuc.edu, lhibbel2@uiuc.edu); and **Arnoud Kamperman**, Corus Strip Products IJmuiden, Direct Sheet Plant (arnoud.kamperman@corusgroup.com)



**Figure 1**

Narrow face mold geometry and CON1D simplification (overlaid on left side in red).

transfer characteristics, the channel width was chosen to be about two-thirds of the diameter of the actual round channel. These two considerations yield a 9 x 17-mm channel and a 41-mm-thick mold. CON1D aims only to model a typical section through the mold and cannot predict variations in the direction around the mold perimeter, such as corner effects.

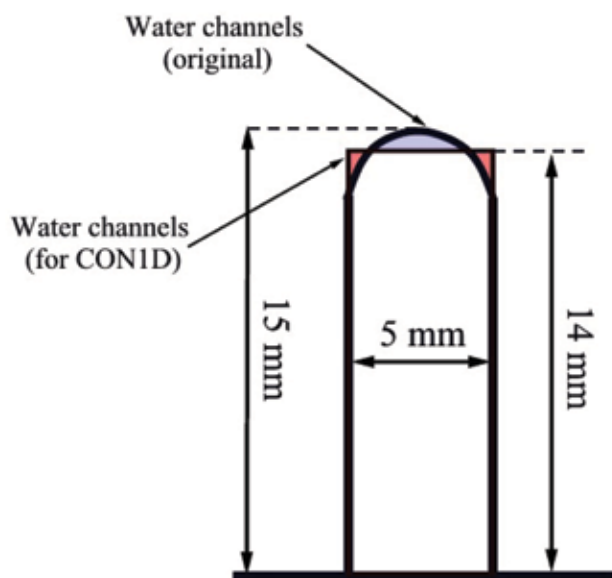
**Wide Face** — Water channels in the wide face required similar dimensional adjustments

for CON1D. The actual water channels are spaced 5 mm apart and are 5 mm wide and 15 mm deep, but with rounded roots. As shown in Figure 2, the CON1D water channels are 5 mm wide but 14 mm deep, so that outer (red) areas compensate for the upper (blue) area and roughly match the real cross-sectional area. The mold thickness was maintained at 35 mm. As shown in Figure 3, this keeps the channels at a constant distance of 21 mm from the hot face, in comparison with the real mold, where the closest point of the rounded channel root is 20 mm from the hot face. The bolt holes have the same dimensions as on the narrow face, but on the wide face the thermocouple holes extend into the mold such that they are 15 mm from the hot face.

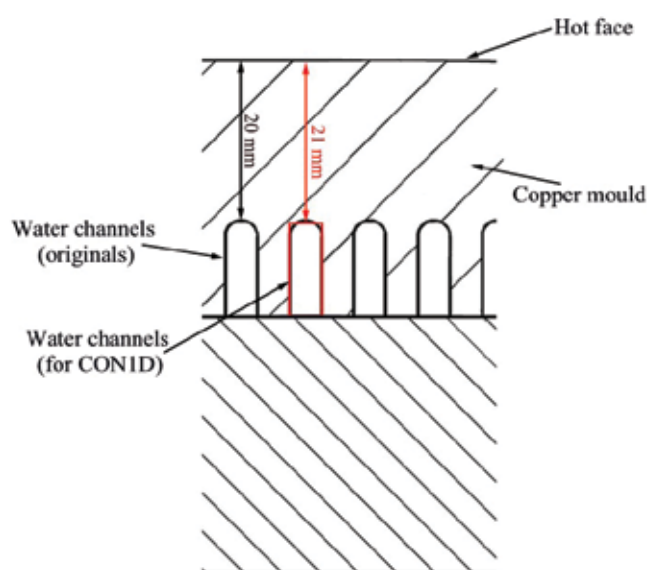
### CON1D Model Offset Determination

To enable CON1D to accurately predict the temperatures of thermocouples, it must be calibrated using a three-dimensional heat transfer calculation, to determine an offset distance for each mold face to adjust the modeled depth of the thermocouples.

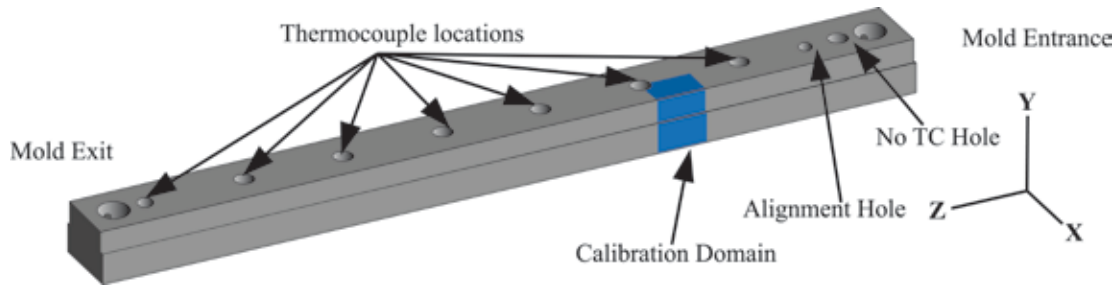
**Narrow Face** — Two different three-dimensional heat transfer models were developed of the mold copper narrow faces (end plates) using ABAQUS 6.6-1. The first was a small, symmetric section of the mold geometry containing one quarter of a single thermocouple, which was used to determine the offset for CON1D. The second was a complete model

**Figure 2**

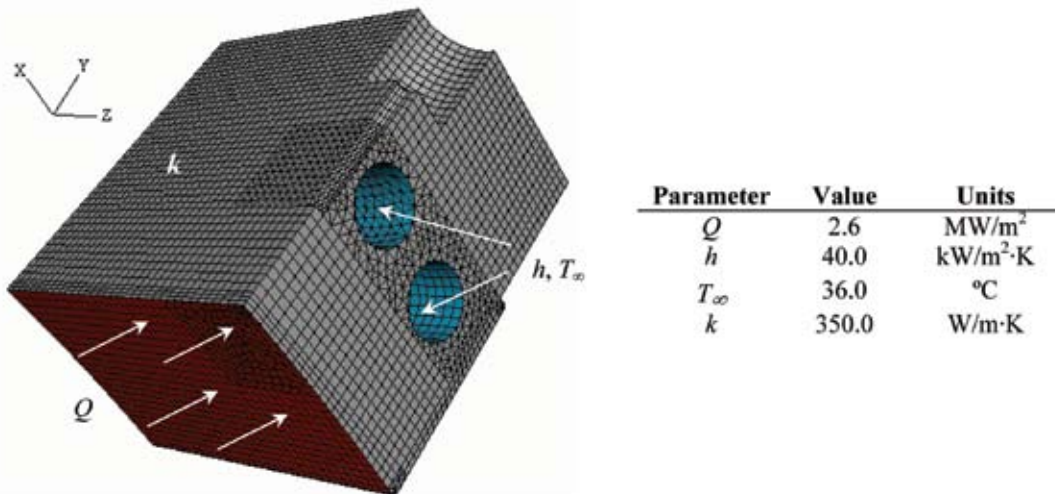
Wide face water slot and CON1D simplification.

**Figure 3**

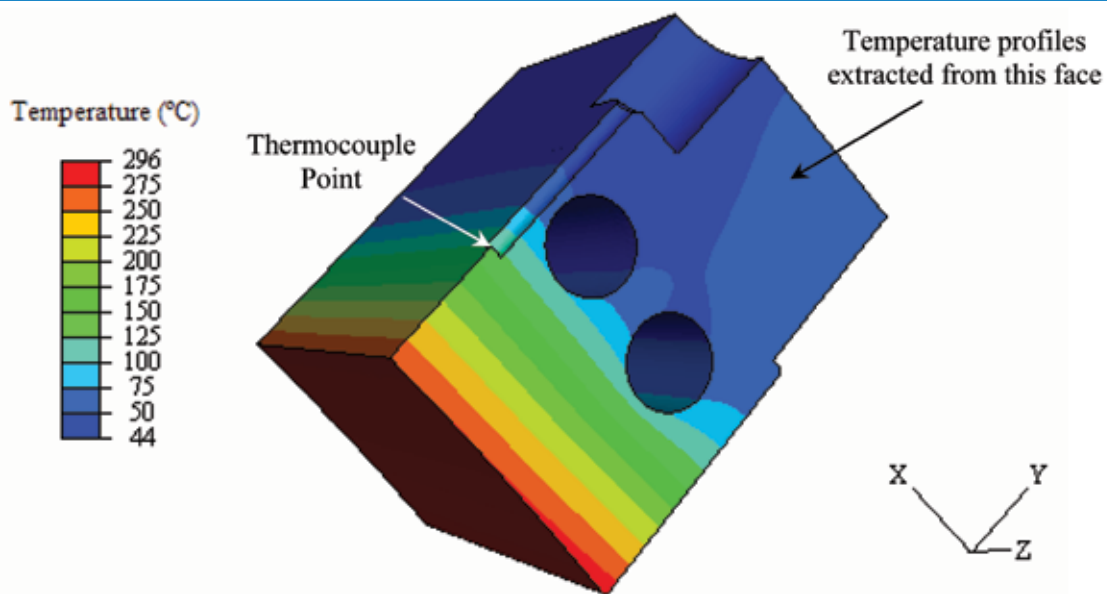
Wide face mold geometry.

**Figure 4**

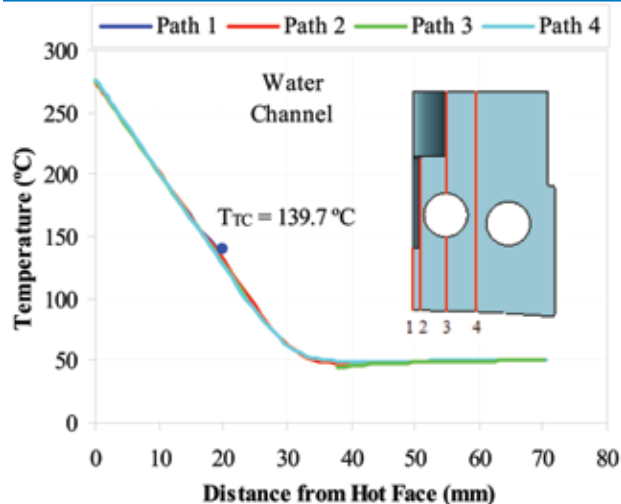
Location of calibration domain.

**Figure 5**

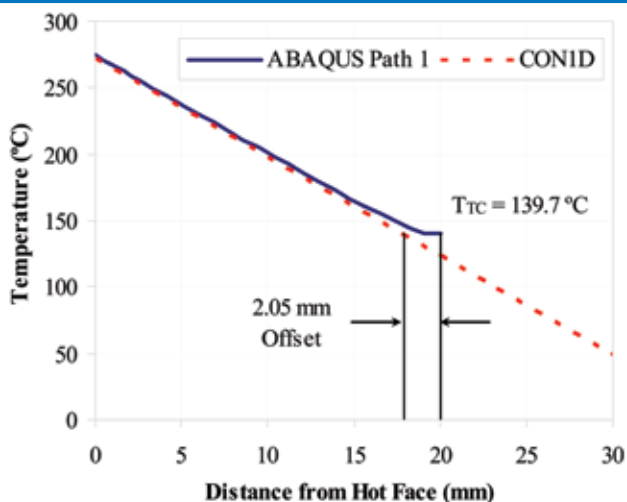
Narrow face boundary conditions and properties.

**Figure 6**

Narrow face calibration results.

**Figure 7**

Temperature profiles in narrow face.

**Figure 8**

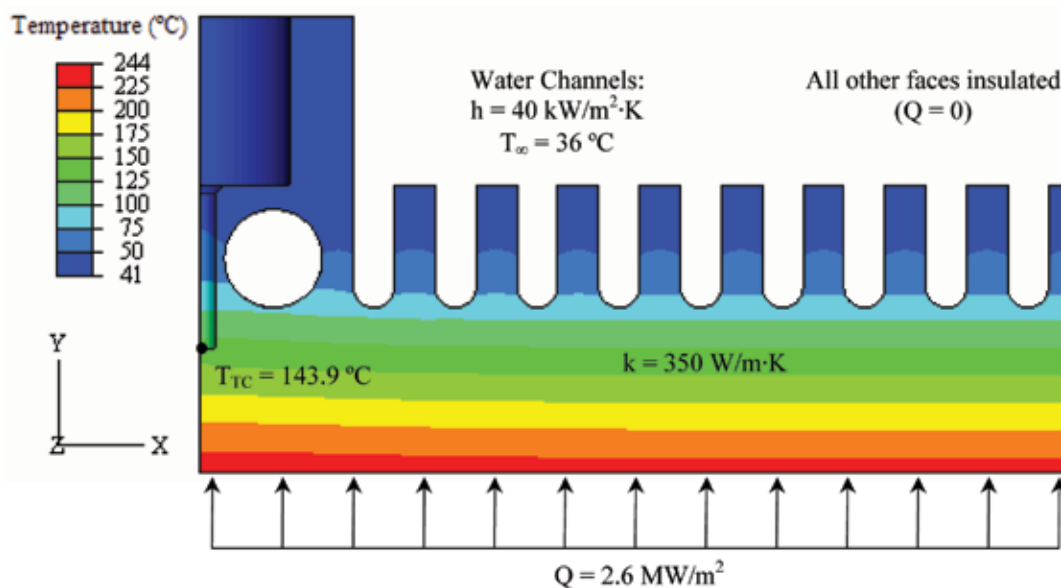
Determination of offset.

of one symmetric half of the entire mold plate, used to determine an accurate temperature distribution, including the effects of all geometric features and to evaluate the CONID model.

To compare properly the finite element model with CONID, identical conditions were applied to both models. Figure 4 highlights the location of this “calibration section” in the entire mold piece, and Figure 5 shows the geometry and simplified boundary conditions. The applied heat flux  $Q$  to the hot face is constant and uniform, as are the thermal conductivity  $k$  of the mold, the convective heat transfer coefficient  $h$  and the water temperature  $T_\infty$  applied to the water channel surfaces. Unlabelled (grey) surfaces are insulated.

The finite element mesh used 45,840 mixed (hexahedrons, tetrahedrons and wedges) quadratic elements and ran in 80 seconds (wall clock) on a 2.0 GHz Intel Core2 Duo PC. Figure 6 shows the resulting temperature contour plot and identifies the location of the thermocouple temperature, as well as the face from which further data were extracted. The maximum temperature of 296°C is found on the hot face corner, which is 20.5°C hotter than the hot face centerline.

The temperature profiles along four paths are shown in Figure 7, in which a linear temperature gradient is evident between the hot face and the water channels. The temperature variation between these paths is small, with

**Figure 9**

Wide face calibration domain with input parameters.

only 2°C difference across the hot face in the vicinity of the paths. The lowest temperature is found on the back (cold face side) of the water channel (Path 3). The missing copper around the thermocouple causes the local temperature to rise about 10°C, however. To account for this effect in CON1D, an offset distance is applied to the simulated depth of the thermocouples.

An offset distance enables the one-dimensional model to accurately relate thermocouple temperatures by accounting for 3-D conduction effects from the complex local geometry.<sup>2</sup> The difference in position between the thermocouples in the mold and in the model is called an “offset” and is the distance the thermocouple position is shifted when input to the CON1D model.

Figure 8 compares the temperature distribution of CON1D with the Path 1 results from Figure 7. Although CON1D cannot capture the localized effects of the complex geometric features, the 3-D thermocouple temperature can be found by “moving” the thermocouple to a new location closer to the hot face. This small “offset distance” allows accurate thermocouple temperatures to be predicted by CON1D. This offset of the thermocouple depth can be determined from Equation 1 using the CON1D temperature profile as follows:

$$d_{\text{offset}} = (T_{TC} - T_{hf}) \frac{dx}{dT} - d_{TC} =$$

$$(139.7 - 273.16)^{\circ}\text{C} \cdot \frac{30\text{ mm}}{(50.21 - 273.16)^{\circ}\text{C}} -$$

$$20\text{ mm} = 2.05\text{ mm}$$

(Eq. 1)

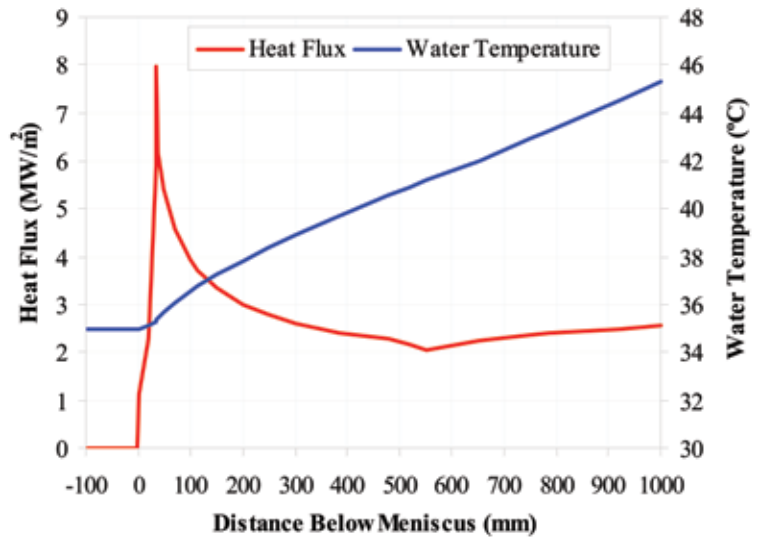
where

$d_{\text{offset}}$  is the offset distance (mm),  
 $T_{TC}$  is the thermocouple temperature from ABAQUS (°C),  
 $T_{hf}$  is the thermocouple temperature from CON1D (°C),  
 $dx/dT$  is the inverse of the temperature gradient from CON1D (mm/°C) and  
 $d_{TC}$  is the actual depth of the thermocouple from the hot face (mm).

Figure 8 also shows that CON1D is able to match the 3-D results for about 12 mm into the mold, or two-thirds of the distance from the hot face to the thermocouple.

**Wide Face** — Following the same procedure used in the narrow face, the offset distance for the wide face was also calculated. The boundary conditions and properties were maintained the same as in the narrow face. A

**Figure 10**



CON1D output heat flux and water temperature profiles as input to ABAQUS.

top view of these conditions and the 3-D temperature distribution is plotted in Figure 9.

The thermocouples in the real wide face are positioned 15 mm from the hot face, and the offset was found to be 2.41 mm, meaning that the thermocouples in CON1D should be 2.41 mm closer to the hot face to produce accurate thermocouple predictions.

### 3-D Mold Temperatures and CON1D Model Verification

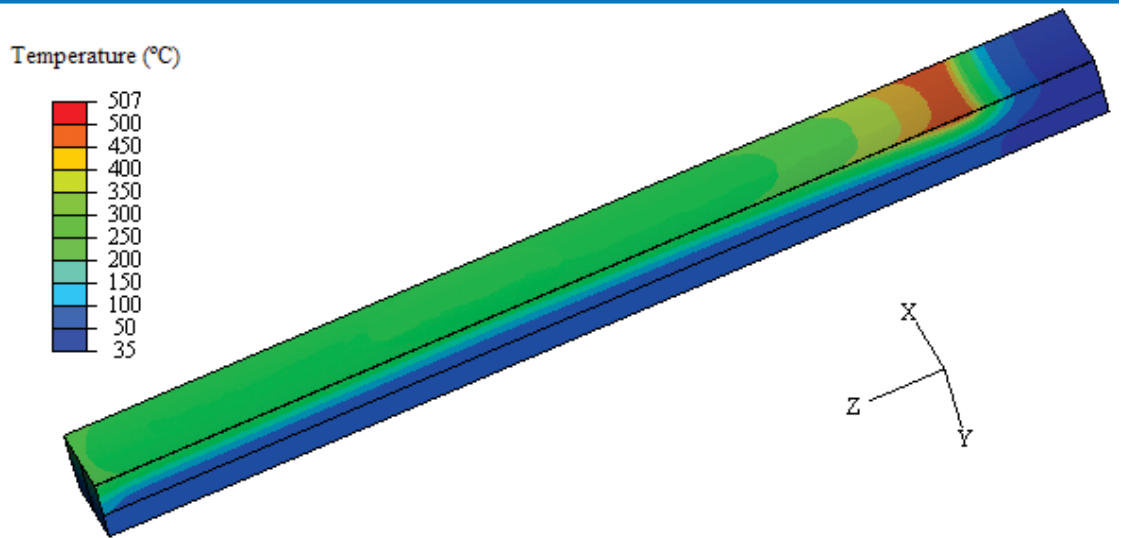
Having calibrated the CON1D model by determining the offset distance, both the full three-dimensional model and CON1D simulation were run using realistic boundary conditions for the mold.

**Narrow Face** — One symmetric half of the entire three-dimensional narrow face geometry was analysed in ABAQUS, using the DFLUX and FILM user subroutines to realistically vary heat flux and water temperature down the mold, as given in Figure 10. Other parameters were maintained as in Figure 5. This ABAQUS model used 468,583 quadratic tetrahedron elements and required 7.1 minutes (wall clock) to analyze.

Figure 11 shows the temperature contours from the three-dimensional model of the entire mold narrow face. Localized three-dimensional effects are observed near the peak heat flux region and at mold bottom. The cooler spot around the center of the hot face corresponds to an inflection point in the heat flux curve. The highest temperatures occur at the small-filleted corners of the mold at the peak heat flux, because they are furthest away from the water channels.

Figure 12 shows the 3-D hot face temperatures extracted along the plane of symmetry



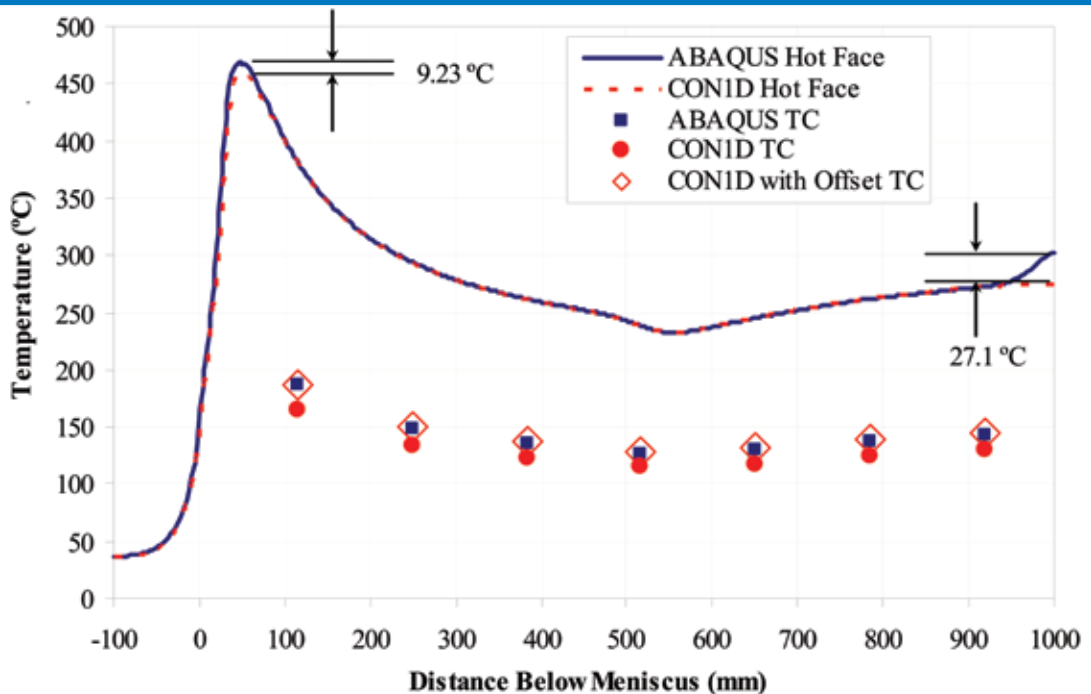
**Figure 11**Full three-dimensional model temperature results ( $^{\circ}\text{C}$ ).

compared with the hot face temperatures from CON1D. The two programs match very well (typically within  $2^{\circ}\text{C}$ ), except around the areas with strong three-dimensional effects. Maximum errors are  $9.2^{\circ}\text{C}$  near the heat flux peak and  $27^{\circ}\text{C}$  at mold bottom, where the water slots end.

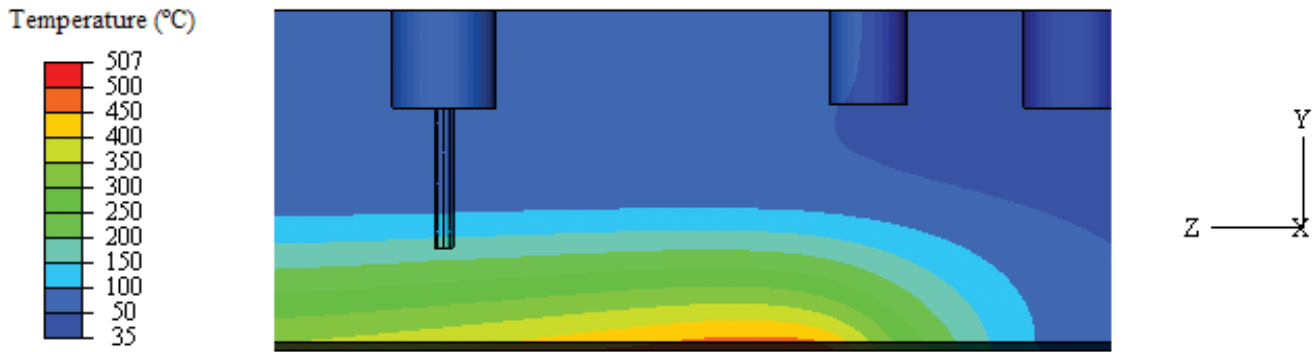
Figure 13 shows the temperature contours around the area of peak heat flux, highlighting the localized thermal effects at this location. Although the CON1D model is least accurate at the hot face at this location, its

two-dimensional mold temperature calculation in the vertical slice allows it to achieve acceptable accuracy.

The temperatures predicted at all seven thermocouple locations in the mold compare closely with the offset CON1D values in Figure 12. The topmost of the eight bolt holes does not have a thermocouple, and the middle hole in Figure 13 is for alignment. The results are tabulated in Table 1 and illustrated in Figure 12. The temperatures match almost exactly (within  $1.4^{\circ}\text{C}$  or less), which is within

**Figure 12**

Hot face and thermocouple temperature comparison between CON1D and ABAQUS.

**Figure 13**

Temperature contours around the peak heat flux.

**Table 1**

### Narrow Face Thermocouple Temperature Comparison

Distance below meniscus (mm)	3-D model	CON1D		CON1D with offset	
	Temperature (°C)	Temperature (°C)	Difference (°C)	Temperature (°C)	Difference (°C)
115	186.6	165.4	-21.2	187.5	0.9
249	148.9	133.6	-15.3	150.0	1.1
383	135.7	122.5	-13.2	136.7	1.0
517	126.3	114.7	-11.6	127.4	1.1
651	129.8	118.0	-11.8	131.1	1.3
785	137.6	124.9	-12.7	139.0	1.4
919	142.9	129.6	-13.2	144.3	1.4

the finite element discretization error. This is a great improvement over the error of 12–21°C produced by CON1D without the offset. Even when the heat flux peak was lowered 80 mm to the level of the first thermocouple to produce maximum 3-D effects, the error in the CON1D prediction for that thermocouple was only -3.4°C. Figure 12 also shows that the CON1D offset method is independent of heat flux, since the same offset was applied to all thermocouples. This means that a given mold geometry needs to be modeled in 3-D only

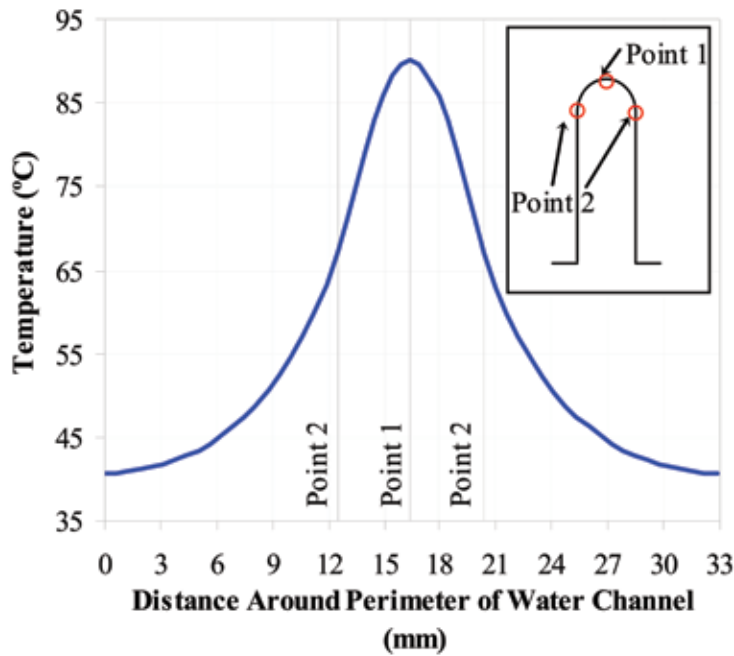
once prior to conducting parametric studies using CON1D. In addition to its increased speed and ease of use, the CON1D model includes powerful additional calculations of the interfacial gap and solidifying shell. Thus, calibrating the CON1D model using the offset method to incorporate the 3-D ABAQUS results, unleashes a powerful and accurate tool to study continuous casting phenomena.

**Wide Face** — In Table 2, ABAQUS and CON1D output results are compared along

**Table 2**

### Wide Face ABAQUS and CON1D Comparison

Parameter	3-D	CON1D
Hot face temperatures	237.2–243°C	237.4°C
Cold face temperatures in the cooling channels:		81.4°C
Point 1: closest point of curved channel root to the hot face	Point 1: 89.44–91.43°C	
Point 2: first straight points after the curve	Point 2: 75.08–77.75°C	
Temperature at the thermocouple location	143.9°C	143.90°C (with offset)

**Figure 14**

Temperature profile around the perimeter of the wide face water channel.

the direction of the mold perimeter at the calibration distance, 219 mm below the meniscus. The temperature at the cold face is tabulated at two points. As expected, point 1 is always hotter (around 90°C) than point 2 (around 76°C). The CON1D predicts the temperature of the water slot root (cold face) to be 81.4°C, which lies in between these two values. Water slot temperatures near the bolt hole are hotter than those near the symmetry

plane. Figure 14 shows the temperature profile around the perimeter of a wide face water channel.

### Validation With Plant Data and Parameter Study

After verifying that the CON1D model matches with the full 3-D model, the next important step is to validate CON1D results with plant data and to check the accuracy of the model under different casting conditions.

**Database Comparison** — A large database of plant data was compared with CON1D simulation results. The database contains more than 700 average values of heat flux, thermocouple temperatures and mold powder consumption, recorded from the wide faces during stable casting periods where the most important casting parameters, including casting speed and slab width, were constant for a period of at least 30 minutes. These data were downloaded from the mold thermal monitoring (MTM) system of the level 2 control system.

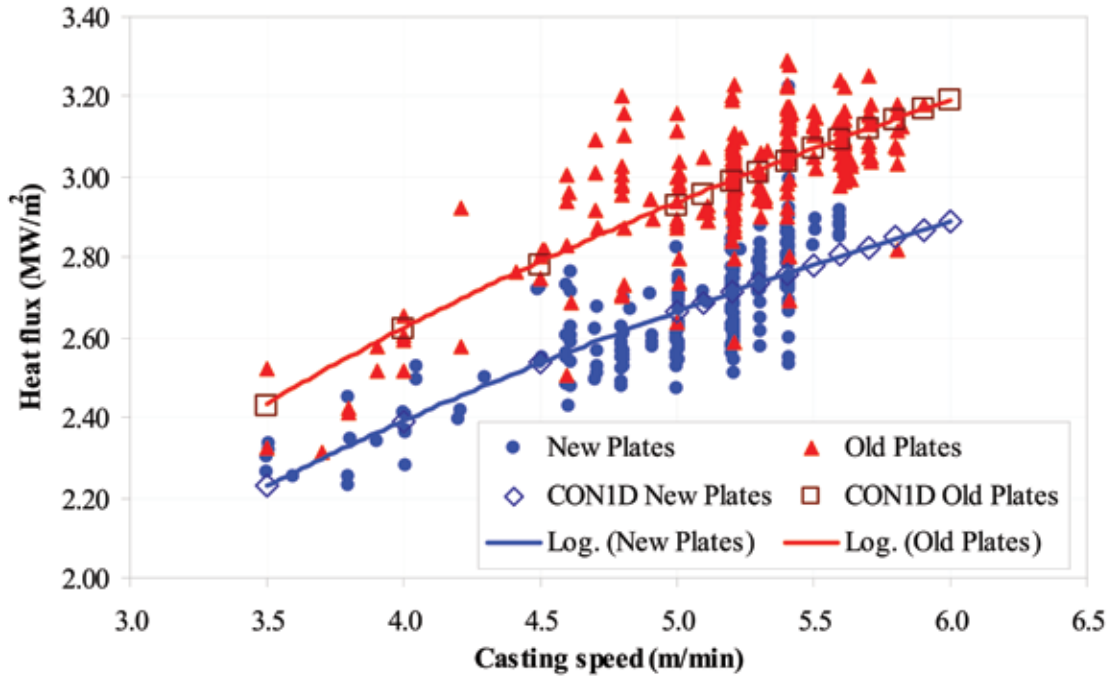
The first comparison with plant data was done for the average mold heat flux (from the cooling water) for different casting speeds. The data were divided according to mold copper thickness into thick new plates (with 0–5 mm mold wear) and thin old plates (with 10–15 mm mold wear). The trend lines match with CON1D predictions, as shown in Figure 15. This match is due partly to the effect of a thinner shell decreasing the thermal resistance at a higher casting speed and a thinner mold lowering the mold thickness, which both

**Table 3**

#### Simulation Conditions

Carbon content, C%	0.045%	Viscosity temp.-dependence exponent, n	2.7
Liquidus temperature, $T_{liq}$	1,531 °C	Slag density, $\rho_{slag}$	2,600 kg/m <sup>3</sup>
Solidus temperature, $T_{sol}$	1,509 °C	Slag absorption factor, a	250 m <sup>-1</sup>
Steel density, $\rho_{steel}$	7,400 kg/m <sup>2</sup>	Slag refractive index, m	1.667
Steel emissivity, $\epsilon_{steel}$	0.8	Slag emissivity, $\epsilon_{slag}$	0.9
Initial cooling water temperature, $T_{water}$	33 °C	Mold powder consumption rate, $Q_{slag}$	0.0714 kg/m <sup>2</sup>
Cooling water velocity, $V_{water}$	8.5 m/s	Pour temperature, $T_{pour}$	1,545 °C
Mold emissivity, $\epsilon_{mold}$	0.5	Slab geometry, width × thickness W × N	1,420 × 70 mm
Mold slag solidification temp., $T_{fsol}$	1,183 °C	Nozzle submergence depth, $d_{nozzle}$	150 mm
Mold slag conductivity, $k_{solid}$ , $k_{liquid}$	1.0, 1.5 W/mK	Oscillation mark geometry, $d_{mark}$ × $w_{mark}$	0.08 × 1.5 mm
Air conductivity, $k_{air}$	0.06 W/mK	Mold oscillation frequency	325 cpm
Slag layer/mold resistance, $r_{contact}$	9.5E-5 m <sup>2</sup> K/W	Oscillation stroke	6.0 mm
Mold powder viscosity at 1,300 °C, $\mu_{1,300}$	0.9 poise		



**Figure 15**

CON1D mean heat flux compared to plant data.

increase heat flux. The realistic input data, given in Table 3, allow CON1D to capture these effects. The match was improved by accounting for the changes in the solid slag layer velocity, as discussed in the next section of this paper. In addition to investigating mold temperatures, shell growth and interfacial phenomena, this calibrated and validated model enables extrapolation to predict behavior at higher casting speeds.

**Velocity Ratio Between Solid Slag Layer and Steel Shell** — The solid slag layer is assumed to move down the mold at a time-averaged velocity (and location: i.e., thickness of the liquid layer). This ratio ranges between zero (if the slag layer is attached to the mold) and the casting speed (if the slag layer is attached to the shell). This ratio between the solid slag speed and the casting speed must be input to the CON1D model. For a given powder consumption rate, this controls the average thickness of the slag layer, which greatly influences mold heat flux. A rough estimate of this ratio is given by:

$$\frac{V_{flux}}{V_C} = \frac{Q_{MP}}{\rho d_{slag}} \quad (\text{Eq. 2})$$

where

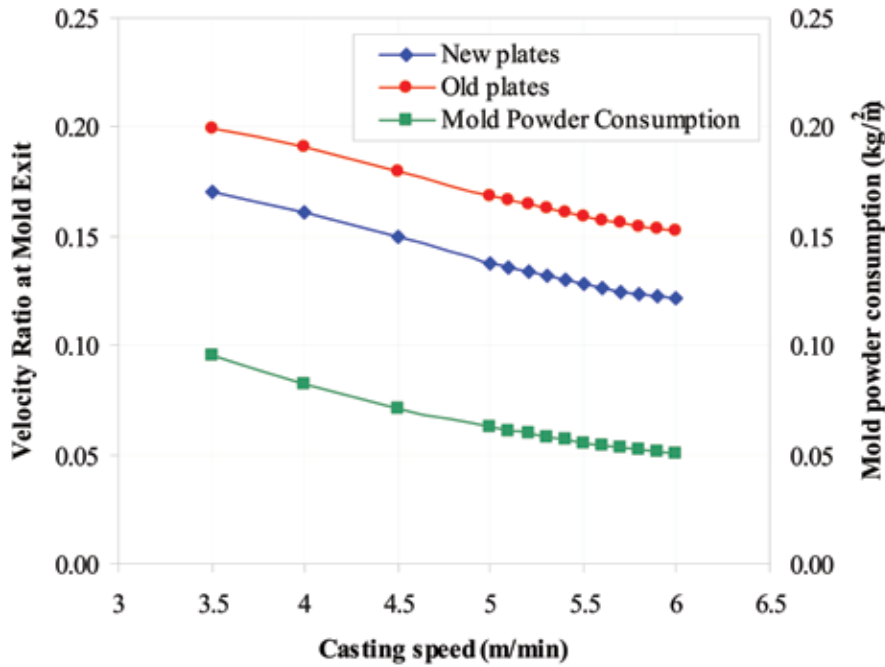
$V_{flux}$  is the velocity of solid slag layer (m/min),  
 $V_C$  is the casting speed (m/min),  
 $Q_{MP}$  is the mold powder consumption (kg/m<sup>2</sup>),

$\rho$  is the mold slag density (kg/m<sup>3</sup>) and  
 $d_{slag}$  is the slag layer thickness (m).

In practice, this velocity ratio varies with distance down the mold, which was characterized in this work to increase linearly between two values. At the meniscus, the ratio is zero, because the solid slag sticks to the mold wall and is relatively undisturbed due to the low friction associated with the liquid slag layer lubrication. At mold exit, Equation 2 is applied, based on the typical thickness of the solid slag layer that was measured at mold exit.

Slag film fragments previously taken from mold exit of the DSP caster ranged from 50 to 500 microns in thickness.<sup>4</sup> Because most of these fragments were split in the longitudinal direction, an average thickness of 200 microns was used in the first approximation of the velocity ratio. Further velocity ratios were found as a function of casting speed for both new and old mold plates, to match the average heat fluxes from the plant data. These two sets of ratios are plotted in Figure 16 and compared with mold powder consumption.

The velocity ratio has a strong correlation with the mold powder consumption, as given in Equation 2. This relation also can be seen in Figure 16, where both velocity ratio curves drop with increasing casting speed in the same way as the mold powder consumption. This finding is logical because a higher casting speed increases both hot face temperature and shell surface temperature in the mold. This encourages a hotter, thicker liquid

**Figure 16**

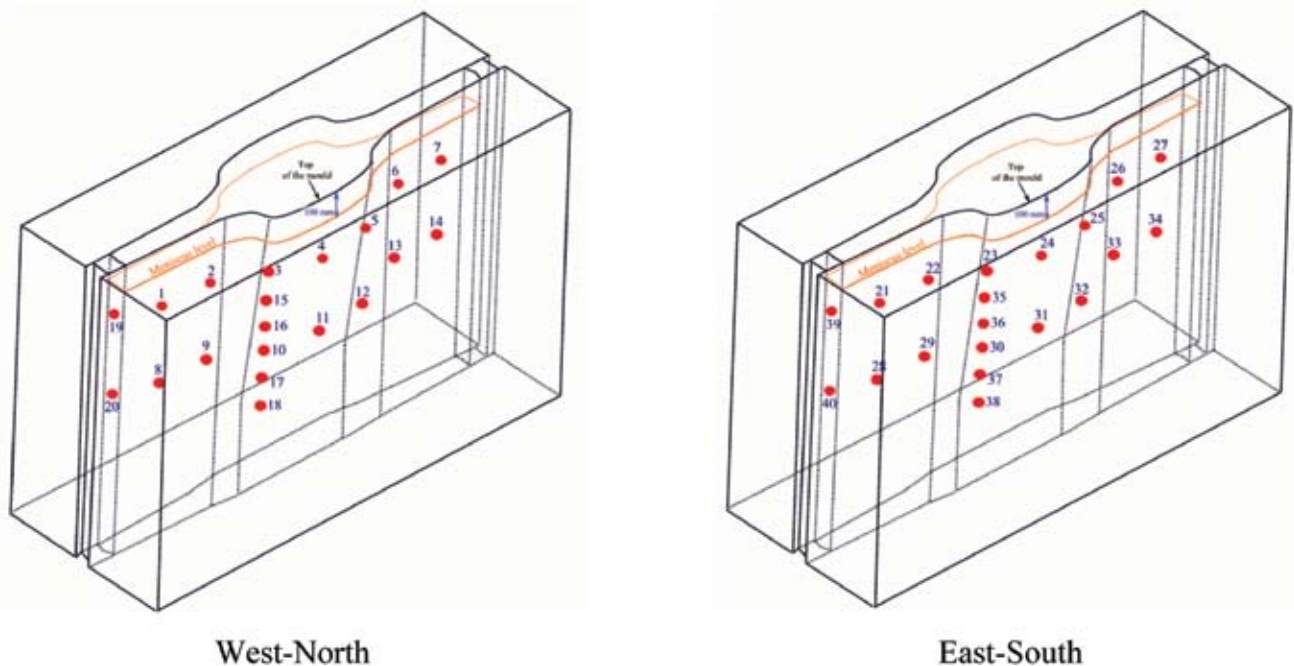
Effect of casting speed on consumption and velocity ratios in new (thick) and old (thin) mold plates.

slag layer, which extends further down the mold, which encourages the solid slag layer to remain more attached to the mold wall, producing a lower velocity. Furthermore, the higher hot face temperature tends to keep the mold slag above its glass transition temperature, making slag fracture less likely and thus

resulting in a lower average velocity ratio at a higher casting speed.

Mold heat flux varies with casting speed, velocity ratio and mold plate thickness. The CON1D results indicate that the velocity ratio itself varies with plate thickness. In new (thicker) plates, the mold hot face temperature is higher, which has a similar effect to increasing casting speed. Thus, the velocity ratio is expected to drop with new thin plates. The actual speed of the moving solid slag layer is not easily measured. Thus, the application of calibrated and validated models such as CON1D is important to achieve the understanding of mold phenomena necessary to extrapolate plant data to new conditions and to solve quality problems.

**Temperature Validation** — Plant data were obtained from a mold instrumented with forty thermocouples, as part of the standard MTM system to further evaluate the CON1D predictions. A period of 23 minutes of stable casting at a speed of 5.2 m/minute and a width of 1,328 mm was chosen for this comparison, due to its stability in the thermocouple measurements. The meniscus level was measured to be 100 mm below the top of the

**Figure 17**

Thermocouple numbers in the DSP mold.

**Table 4****Thermocouples Used in the Comparison With Plant Data**

Row	Thermocouple number	Distance below meniscus (mm)
1	2, 3, 4, 5, 6, 22, 23, 24, 25, 26	75
2	15, 35	200
3	16, 36	325
4	9, 10, 11, 12, 13, 29, 30, 31, 32, 33	450

mold. The thermocouple numbers and positions are listed in Table 4 and shown in Figure 17. Their 15-mm depth below the hot face was offset by 2.41 mm to 12.59 mm for CONID.

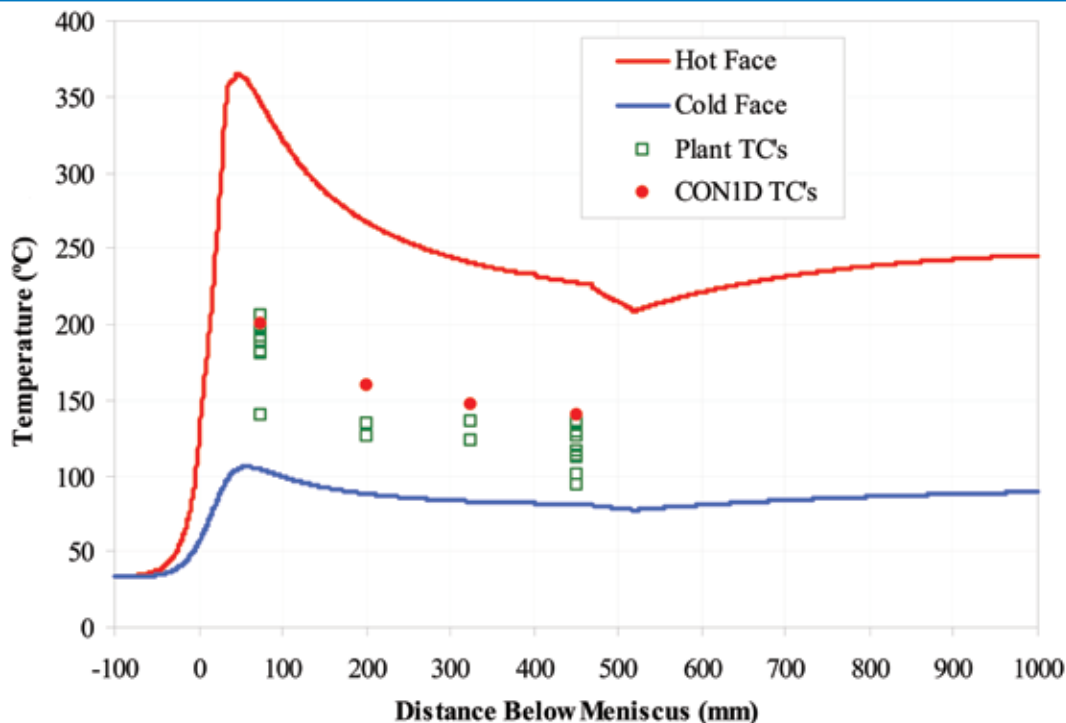
The predicted hot face temperature profile, cold face (water slot root) temperature profile and thermocouple temperatures from CONID are shown in Figure 18. This figure also shows the average of the measured temperatures, which are slightly lower. This might be due to minor contact problems causing the thermocouple temperatures to drop, or if boiling in the water channels caused the mold temperature to drop. Scale formation in the water channels would cause the mold temperature to be too high.

**Parametric Study** — The verified, calibrated and validated CONID model is being applied to investigate a range of mold thermal phenomena, including high-speed casting, mold

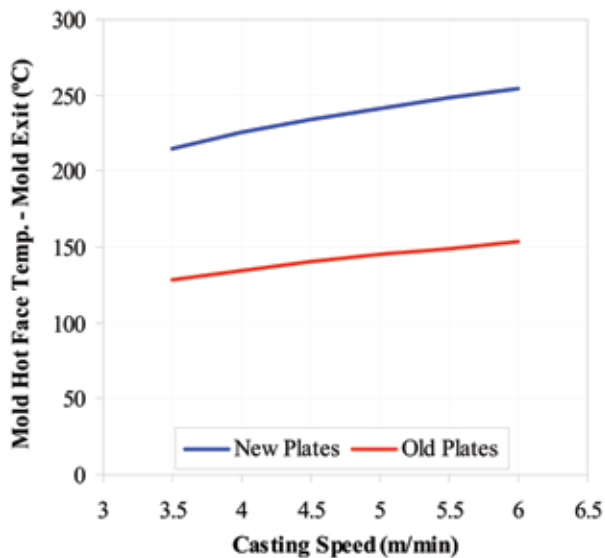
powder properties, scale formation in the water channels and breakout prediction. The effect of mold plate thickness on interfacial gap phenomena is investigated in the following section.

The effect of casting speed and mold plate thickness on various parameters at mold exit are shown in Figures 19–22. Increasing casting speed naturally increases the mold hot face temperature and decreases the shell thickness. This causes the slab surface temperature to increase, although the increased heat flux with increasing casting speed tends to counter this trend. Slag layer thickness decreases with casting speed, owing to the smaller slag consumption rate, but the opposing effect of lower solid slag velocity ratio tends to lessen this trend.

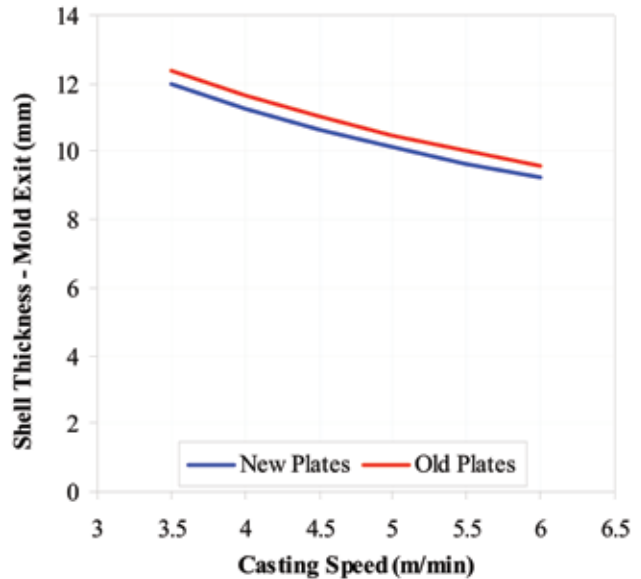
Increasing the mold plate thickness (with new plates) naturally increases the hot face temperature. This lowers the solid slag layer

**Figure 18**

Predicted thermocouple temperature compared with plant data in the considered period.

**Figure 19**

Effect of casting speed on mold hot face temp.

**Figure 20**

Effect of casting speed on shell thickness.

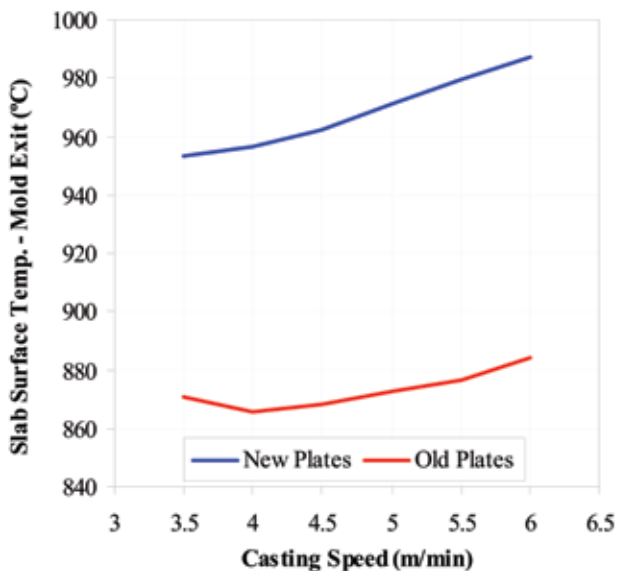
velocity (Figure 16), which produces a thicker slag layer, as shown in Figure 22. Together with the extra resistance of the thicker mold plate, this decreases the heat flux. This causes the shell thickness to decrease and slab surface temperature to increase.

### Conclusions

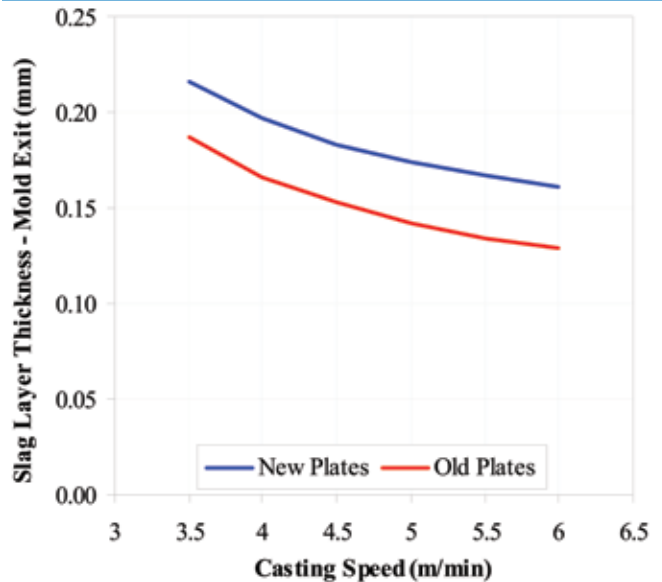
This work summarizes the development of an accurate computational tool for modeling heat transfer in the thin slab continuous casting mold at the Corus DSP. Work toward this end includes model verification with a

complete thermal 3-D analysis of the entire complex mold geometry, model calibration using the offset method to match thermocouple measurements, and model validation with more than 700 sets of plant data from an instrumented mold. The CON1D model is then applied together with plant measurements to gain a new insight into the effects of casting speed and mold plate thickness on mold heat transfer. Project findings include:

- Increasing casting speed causes a thinner solidified steel shell, higher heat

**Figure 21**

Effect of casting speed on slab surface temperature.

**Figure 22**

Effect of casting speed on slag layer thickness.

flux, higher mold hot face temperature, a thinner slag layer and lower solid slag layer velocity.

- Increasing mold plate thickness increases hot face temperature, lowers solid slag layer velocity, increases slag layer thickness and lowers mold heat flux.

The CON1D model is being applied to gain further insight into continuous casting of thin slabs, including the extrapolation of model predictions of heat transfer and interfacial phenomena to higher casting speed and the optimization of mold taper, mold distortion and funnel design.

## Acknowledgments

The authors wish to thank the member companies of the Continuous Casting Consortium and the National Science Foundation (Grant # 05-00453) for support of this work, the National

Center for Supercomputing Applications for computational resources, and personnel at Corus DSP for plant data and support.

## References

1. Y. Meng and B.G. Thomas, "Heat Transfer and Solidification Model of Continuous Slab Casting: CON1D," *Metallurgical & Materials Transactions*, Vol. 34B, No. 5, Oct. 2003, pp. 685–705.
2. M. Langeneckert, "Influence of Mould Geometry on Heat Transfer, Thermocouple and Mould Temperatures in the Continuous Casting of Steel Slabs," master's thesis, University of Illinois at Urbana-Champaign, 2001.
3. ABAQUS 6.6-1. 2006, ABAQUS Inc., 166 Valley St., Providence, RI 02909-2499.
4. J.A. Kromhout, S. Melzer, E.W. Zinngrebe, A.A. Kamperman and R. Boom, "Mould Powder Requirements for High-Speed Casting," *Proc. 2006 Int. Symposium on Thin Slab Casting and Rolling*, Guangzhou, 2006, The Chinese Society for Metals, pp. 306–313. ♦

*This paper was presented at AISTech 2007 — The Iron & Steel Technology Conference and Exposition, Indianapolis, Ind., and published in the AISTech 2007 Proceedings.*



Did you find this article to be of significant relevance to the advancement of steel technology? If so, please consider nominating it for the AIST Hunt-Kelly Outstanding Paper Award at [www.aist.org/huntkelly](http://www.aist.org/huntkelly).

**FPO - 1/2 horiz.**